Electron collisions with ethylene: The role of multichannel-coupling effects

Romarly F. da Costa,[1,2,*] Márcio H. F. Bettega,[3] Márcio T. do N. Varella,[4] Eliane M. de Oliveira,[2] and Marco A. P. Lima[2]

[1]*Centro de Ciências Naturais e Humanas, Universidade Federal do ABC, 09210-580 Santo André, São Paulo, Brazil*

[2]*Instituto de Física "Gleb Wataghin," Universidade Estadual de Campinas, 13083-859 Campinas, São Paulo, Brazil*

[3]*Departamento de Física, Universidade Federal do Paraná, CP 19044, 81531-990 Curitiba, Paraná, Brazil*

[4]*Instituto de Física, Universidade de São Paulo, CP 66318, 05315-970 São Paulo, São Paulo, Brazil*

(Received 5 September 2014; published 10 November 2014)

We report integral and differential cross sections for elastic and electronically inelastic ($X\,^1A_g \rightarrow \tilde{a}\,^3B_{1u}$) electron scattering by ethylene. The Schwinger multichannel method with pseudopotentials in the N_{open}-channel-coupling scheme at the static-exchange-plus-polarization approximation is employed to calculate the scattering amplitudes at impact energies ranging from 5.7 to 50 eV. We discuss the multichannel-coupling effects in the calculated cross sections, in particular, how the number of excited states included in the open-channel space impacts the convergence of the elastic and the ($X\,^1A_g \rightarrow \tilde{a}\,^3B_{1u}$) excitation cross sections at higher collision energies. We found good agreement between the present calculated total cross section (which includes elastic, inelastic, and ionization contributions, the latter estimated with the binary-encounter-Bethe model) and the experimental data.

DOI: 10.1103/PhysRevA.90.052707 PACS number(s): 34.80.Bm, 34.80.Gs

I. INTRODUCTION

The scattering of low-energy electrons by the ethylene molecule has been the subject of a considerable number of investigations, especially compared to collision processes involving other polyatomic species. The total cross section (TCS) data set consists of the absolute measurements by Brüche [1], Floeder *et al.* [2], Nishimura and Tawara [3], and Szmytkowski *et al.* [4] and of the normalized data reported by Sueoka and Mori [5] and Lunt *et al.* [6]. These results agree in shape and with respect to the determination of two maxima, although they show differences in the magnitude of the TCSs. The study of elastic electron scattering by ethylene has recently been addressed by both experimental [7–9] and theoretical [10,11] groups. In particular, it has been shown that the *ab initio* calculations can only accurately reproduce the behavior of the experimental differential cross sections (DCSs) for energies below 5 eV through the inclusion of electronic correlation and polarization effects. On the other hand, quantitative disagreement between measured and calculated DCSs was found at intermediate incident energies (20 and 30 eV), clearly showing that the inclusion of another important effect is probably missing. Target distortion effects have also been shown to be important for the proper description of the electronic excitation of ethylene by electron impact. In fact, the agreement between theory [12,13] and experiment [13] for the electronic excitation of the $\tilde{a}\,^3B_{1u}$ state at 5.7 and 7 eV is very good and it was only obtained by the inclusion of polarization effects. The importance of polarization effects on electronic excitation of molecules containing low-energy electronic states around shape resonances was first discussed for furan [14], and then the inclusion of these effects made theory agree with experiments just above the threshold for ethylene [12,13]. These molecules have in common the presence of shape resonances that lie, above the first triplet threshold, at the static-exchange approximation and, below it, at the static-exchange-plus-polarization (SEP) approximation. The proper balance of polarization forces was essential to obtain electronic excitation cross sections of these low-lying triplet states in agreement with experiments. This fact was not considered in previous studies on electronic excitation of ethylene [16,17]. Later, the importance of this polarization dynamics [14] was also confirmed for furan, due to its good agreement with new experiments [15]. In a recent work, Do *et al.* [18] extended the energy range in which experiments involving the $X\,^1A_g \rightarrow \tilde{a}\,^3B_{1u}$ electronic transition by electron impact were available by measuring DCSs from 9 to 50 eV. Their results were in good agreement with the data previously measured by Allan *et al.* [13] but were significantly lower in magnitude compared to the calculated DCSs. Due to the discrepancies mentioned above, in what follows we discuss the influence (and rate of convergence) of multichannel coupling on the electron scattering cross sections of the elastic and of the electronic excitation of the $\tilde{a}\,^3B_{1u}$ channels of ethylene.

The paper is outlined as follows. In Sec. II the theory is briefly described, while in Sec. III details of our computational procedures are given. Results and discussion are presented in Sec. IV. Finally, in Sec. VI some concluding remarks from this investigation are summarized.

II. THEORY

The Schwinger multichannel (SMC) method [19] is a variational approach to the scattering amplitude. In our calculations we use the parallel version [20] of the SMC implementation that allows the use of norm-conserving pseudopotentials [21] and of single-excitation configuration interaction techniques for target description [22]. Since the method [22] and its computational implementation have been described in detail elsewhere, here we only give the working expression for the scattering amplitude,

$$f(\mathbf{k}_f,\mathbf{k}_i) = -\frac{1}{2\pi}\sum_{m,n}\langle S_{\mathbf{k}_f}|V|\chi_m\rangle(d^{-1})_{mn}\langle\chi_n|V|S_{\mathbf{k}_i}\rangle, \quad (1)$$

*romarly.costa@ufabc.edu.br

where

$$d_{mn} = \langle \chi_m | \left[\frac{\hat{H}}{N+1} - \frac{\hat{H}P + P\hat{H}}{2} + \frac{PV + VP}{2} - VG_P^{(+)}V \right] | \chi_n \rangle \quad (2)$$

In the expressions above, P is a projector onto N_{open} energy-allowed target electronic channels, i.e.,

$$P = \sum_{\ell=1}^{N_{\text{open}}} |\Phi_\ell\rangle\langle\Phi_\ell|, \quad (3)$$

$G_P^{(+)}$ is the free-particle Green's function projected onto the P space, V is the projectile-target interaction potential, $\mathbf{k}_i$ ($\mathbf{k}_f$) is the incoming (outgoing) projectile wave vector, and $\hat{H} = E - H$ is the collision energy minus the scattering Hamiltonian. The latter is given by $H = H_0 + V$, where H_0 describes the noninteracting electron-molecule system and $S_{\mathbf{k}}$ is a solution of H_0, namely, the product of a plane wave (projectile) and the target ground state. For the expansion of the variational scattering wave function, the method employs trial basis sets comprising $(N+1)$–particle configuration state functions denoted χ_m and built from antisymmetrized products of target electronic states and projectile scattering orbitals. The open electronic collision channels are included in the P space and the dynamical response of the target electrons to the projectile field (correlation-polarization effects) is accounted for through virtual excitations of the target. In this case, the configuration state functionss are given by

$$|\chi_m\rangle = \mathcal{A}_{N+1}|\Phi_i(1,\ldots,N)\rangle \otimes |\varphi_j(N+1)\rangle, \quad (4)$$

where $i > 0$ and $|\Phi_i\rangle \equiv {}^{(2S+1)}(h_i \rightarrow p_i)$ is a singly excited state obtained by promoting one electron from a hole orbital (h_i) to a particle orbital (p_i), with either singlet ($S = 0$) or triplet ($S = 1$) spin coupling, though only $(N+1)$-electron configurations with total spin $S = 1/2$ (doublets) are actually taken into account. This level of calculation is called as the N_{open}-channel-coupling scheme at the SEP (N_{open}ch-SEP) approximation.

We also employed the binary-encounter-Bethe (BEB) model [23] to estimate the total ionization cross section by electron impact of ethylene. This cross section, added to our computed elastic + inelastic cross section, is compared to the TCS data. This model provides the following expression for the ionization cross section per molecular orbital:

$$\sigma_{\text{BEB}}(T) = \frac{S}{t+u+1}\left[\frac{\ln t}{2}\left(1 - \frac{1}{t^2}\right) + 1 - \frac{1}{t} - \frac{\ln t}{t+1}\right]. \quad (5)$$

In the above expression T is the incident electron energy, $t = T/B$ and $u = U/B$ are normalized energies, where B and U are the orbital binding and electron kinetic energy, respectively, $S = 4\pi a_0^2 N_{\text{occ}} R^2/B^2$, where N_{occ} is the orbital occupation number, $a_0 = 0.5292$ Å, and $R = 13.61$ eV. The total ionization cross section is obtained by the summation of $\sigma_{\text{BEB}}(T)$ over the molecular orbitals satisfying $T > B$. This model provides ionization cross sections which agree with the experiment within 5%–15% (considering different molecules), for incident energies ranging from the first ionization threshold to several kilo–electron volts [24].

III. COMPUTATIONAL PROCEDURES

In order to maintain control over some, of the many possible, variables that affect the description of the electron-molecule collision problem (Cartesian Gaussian basis set, configuration space, target description, multichannel coupling, quadrature scheme, angular momentum expansion), we decided to carry out this new round of calculations for ethylene with the same procedures as adopted in Ref. [12], except with regard to the composition of the single-excitation configuration space used for target description and, accordingly, the level of channel coupling involved in the scattering calculations. As in our previous work, the target was treated as a D_{2h} symmetry-group molecule. Here it is important to note that though many of the excited states included in the scattering calculations have geometries (comprising the appropriate symmetry breaking due to the geometrical distortion) which are different from the ground-state geometry, the absence of resonances in the energy range considered in this work legitimates the use of the fixed-nucleus approximation. The ground and excited states of ethylene were described at the Hartree-Fock level employing the Cartesian Gaussian basis sets given in Ref. [12], which leads to 90 uncontracted functions. The virtual orbitals obtained within the Hartree-Fock approximation were then mixed to produce singlet- and triplet-coupled improved virtual orbitals. Through the use of these improved virtual orbitals, we constructed a minimal orbital basis for a single configuration interaction (MOBSCI) [22] composed of 22 pairs of hole-particle orbitals which is capable of nearly reproducing the spectrum obtained with a full single-configuration-interaction (FSCI) calculation for energies below 10 eV. A summary of the spectrum of excitation energies obtained within MOBSCI and FSCI levels of approximation along with the corresponding experimental assignments is reported in Table I. For the sake of completeness, in Table II we also present a list of all 44 excited states (where 16 of them are physical states and the others are pseudostates) obtained according to the MOBSCI strategy as well as the main hole-particle contributions to the specific transition and the corresponding excitation threshold. The configuration state functions space for the scattering calculations also is of approximately the same size as those used in Ref. [12] and was constructed with modified virtual orbitals (in addition to the active particle orbitals of the MOBSCI) in order to better account for polarization effects. It is noteworthy that the configuration space is the same for all N_{open}ch-SEP approximations (that is, for calculations with $N_{\text{open}} = 1,2,\ldots,45$, where more collision channels are open as the collision energy increases). Finally, we should mention that the 2ch-SEP cross sections obtained with this procedure are in close agreement with those previously reported [12], pointing out that the effect which is discussed arises only from the different channel-coupling schemes used in the present study. The binding and kinetic energies appearing in Eq. (5) were calculated using GAMESS [25] in a restricted Hartree-Fock calculation with a 6-311G++$(2d,1p)$ basis set at the same equilibrium geometry used in the SMC calculations. With these considerations in mind we are now prepared

TABLE I. Calculated and experimental excitation energies for ethylene. Up to 20, 30, and 50 eV, the FSCI spectrum is composed of 138, 260, and 402 electronically excited states, respectively. The MOBSCI calculations at these energies were performed with 45 excited states, of which 17 of them are physical (the ground state, 7 singlets, and 9 triplets) states and the others are pseudostates.

	Energy (eV)		
	FSCI	MOBSCI	Expt.
Triplet	3.56	3.60	4.36[a]
	6.90	6.92	6.98[a]
	7.73	7.75	7.79[a]
	8.48	8.83	8.15[b]
	8.80	9.08	8.57[b]
	9.06	9.19	
	9.42	9.58	
	9.48	9.73	
	9.54	9.74	
Singlet	7.11	7.13	7.11[b]
	7.83	7.85	7.80[b]
	7.88	8.55	7.90[b]
	8.99	9.28	8.28[a]
	9.24	9.37	8.62[b]
	9.25	9.54	8.90[a,b]
	9.63	9.71	9.10[a]
			9.33[a]
			9.51[a,c]
			9.62[a]

[a]Experimental data from Ballard *et al.* [26].
[b]Experimental data from Do *et al.* [18].
[c]For this energy two states were found.

TABLE II. Calculated excitation energies for ethylene obtained according to the MOBSCI strategy at the 45-channel level of approximation. Among these states, 16 of them are physical excited singlets or triplet states that reproduce the FSCI spectra below 10 eV, and the 28 remaining states are pseudostates.

	Hole → particle pair	Energy (eV)	
Symmetry	(main contribution)	Triplet	Singlet
A_g	$(b_{3u} \rightarrow b_{3u})$	9.73	11.94
B_{1u}	$(b_{3u} \rightarrow b_{2g})$ and $(b_{3g} \rightarrow b_{2u})$	3.60	8.55
		12.24	14.13
		14.81	16.58
B_{2u}	$(b_{3g} \rightarrow b_{1u})$	13.25	14.08
B_{3g}	$(b_{3g} \rightarrow a_g)$	11.70	12.34
B_{3u}	$(b_{3u} \rightarrow a_g)$ and $(a_g \rightarrow b_{3u})$	6.92	7.13
		9.08	9.28
		10.56	10.96
		10.98	12.46
		15.88	16.22
		16.23	17.33
B_{2g}	$(b_{3u} \rightarrow b_{1u})$ and $(a_g \rightarrow b_{2g})$	7.75	7.85
		9.58	9.71
		9.74	10.45
		13.05	13.22
		13.29	14.14
		16.83	17.91
B_{1g}	$(b_{3g} \rightarrow b_{2g})$ and $(b_{3u} \rightarrow b_{2u})$	8.83	9.37
		9.19	9.54
		11.85	12.24
A_u	$(b_{3u} \rightarrow b_{3g})$	11.93	12.15

to investigate the influence of the multichannel coupling on elastic and electronically inelastic electron scattering by ethylene. Finally, it is also important to note that, since ionization channels are indeed just electronic excitations to the continuum, their proper inclusion (through a more robust scattering-wave configuration space and by a specific Green function in the SMC method) would affect the collision process and add competing channels for the scattered flux. In the present situation we have just added an approximate contribution to the TCS.

IV. RESULTS AND DISCUSSION

Figures 1–3 show the DCSs calculated at different levels of multichannel coupling. More specifically, the results obtained at the 1ch-SEP, 2ch-SEP, 3ch-SEP, 8ch-SEP, 17ch-SEP, and 45ch-SEP levels of approximation are presented for a representative set of energies contained in the range from 5.7 up to 50 eV. As shown in Fig. 1, the agreement of our elastic DCSs with available experimental data is consistently improved as the channel coupling increases from the 1ch-SEP [dotted (blue) line] to the 45ch-SEP (thick solid black line) approximation. Moreover, the great similarity of the curves corresponding to the 17ch-SEP [solid (violet) line] and the 45ch-SEP approximations, in addition to the excellent agreement with the experimental measurements, provides a strong indication that a good convergence with respect to multichannel coupling has been achieved to the elastic channel. It is also interesting to note that in the intermediate angular region (from 30° to 150°) the DCSs are much more sensitive to the number of channels included in the calculation. Figure 2 shows the DCSs for the electronic excitation of the $\tilde{a}\,^3B_{1u}$ state of ethylene by electron impact at the energies of 5.7, 7, 9, and 11 eV. For the energies of 5.7 and 7 eV the DCSs obtained within the 2ch-SEP approximation are in very good agreement with the experimental results in Ref. [13]. As explained in detail elsewhere [12,13], in this case the agreement is obtained due to a proper balance between the contributions of multichannel and polarization effects. For the energy of 7 eV we note that, although the shape of the backward scattering in the DCS obtained at the 3ch-SEP (long-dashed black line) approximation has been improved, the magnitude at this angular region is still slightly below the experimental data. At the energies of 9 and 11 eV the calculated and measured DCSs do not agree satisfactorily, even when all possible open states (in the present MOBSCI) are included in the target projector P. At 9 eV the DCSs obtained with 2ch-SEP and 8ch-SEP approximations are similar to each other and about a factor of 3 higher than the experimental data in Ref. [18]. It is somewhat disappointing that the results obtained at relatively different levels of multichannel coupling are so close to each other and far away from experimental values. For the energy of 11 eV, the DCSs obtained at the 2ch-SEP and the 17ch-SEP approximations are very close to each other and agree with the experiments in Refs. [13,18] at 0° and above 90°. Between

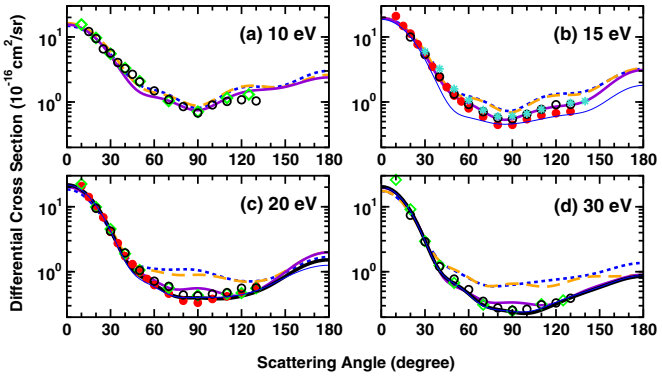

FIG. 1. (Color online) Differential cross sections for elastic electron scattering by ethylene molecules at incident energies of (a) 10 eV, (b) 15 eV, (c) 20 eV, and (d) 30 eV. Dotted (blue) line, 1-channel coupling plus polarization; dashed (orange) line, 2-channel coupling plus polarization; solid (violet) line, 17-channel coupling plus polarization; thick solid black line, 45-channel coupling plus polarization; and thin solid (blue) line, 45-channel coupling plus polarization with ficticious thresholds (see text for details). Open (green) diamonds, open black circles, (turquoise) asterisks (at 15.5 eV), and filled (red) circles: experiments from Refs. [7–9,27], respectively.

0° and 90° theoretical and experimental results display quite different shapes, disagreeing with each other by a factor of $\lesssim 3$. The results presented in Fig. 3 show that the inelastic DCSs are strongly influenced by the multichannel-coupling effects, especially for the impact energies of 30, 40, and 50 eV. The cross sections obtained in the 45ch-SEP approximation are one order of magnitude smaller and about a factor of 2 lower than the results for the 2ch-SEP and the 17ch-SEP approximations, respectively. For the energies of 30 and 50 eV, the DCS obtained from our most sophisticated calculation (45ch-SEP) is still about a factor of 3 above the experimental data in

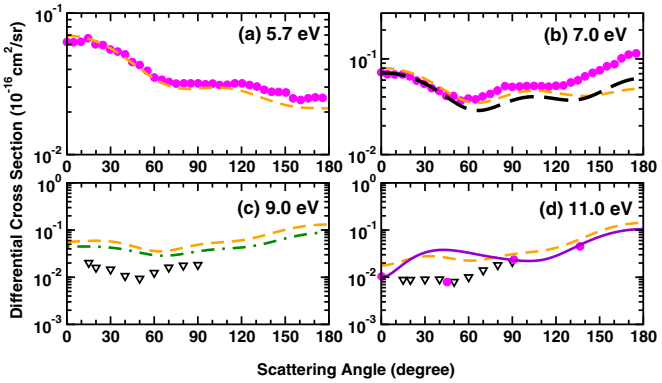

FIG. 2. (Color online) Differential cross sections for the $X\,^1A_g \rightarrow \tilde{a}\,^3B_{1u}$ electronic transition of the ethylene molecule for electron impact energies of (a) 5.7 eV, (b) 7 eV, (c) 9 eV, and (d) 11 eV. Dashed (orange) line, 2-channel coupling plus polarization; long-dashed black line, 3-channel coupling plus polarization; dashed-dotted (dark-green) line, 8-channel coupling plus polarization; solid (violet) line, 17-channel coupling plus polarization. Filled (magenta) circles and open black downward triangles: experiments Refs. [13,18], respectively.

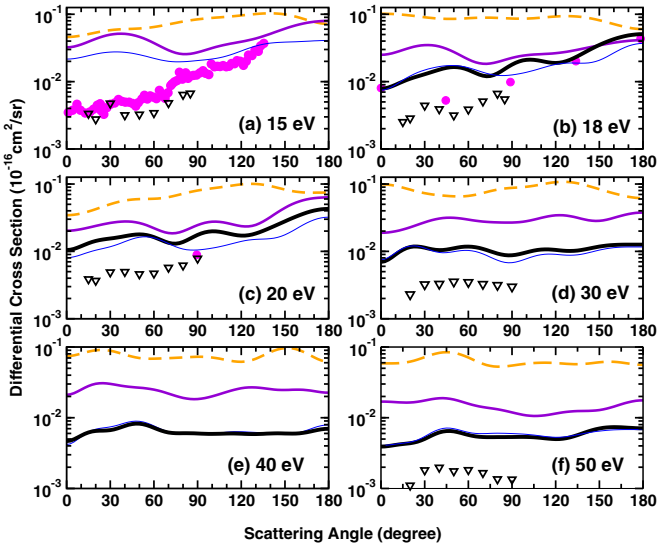

FIG. 3. (Color online) Same as Fig. 2, but at electron impact energies of (a) 15 eV, (b) 18 eV, (c) 20 eV,(d) 30.0 eV, (e) 40.0 eV, and (f) 50.0 eV. Dashed (orange) line, 2-channel coupling plus polarization; solid (violet) line, 17-channel coupling plus polarization; thick solid black line, 45-channel coupling plus polarization; thin solid (blue) line, 45-channel coupling plus polarization with ficticious thresholds (see text for details). Filled (magenta) circles and open black triangles: experiments of Refs. [13,18], respectively, both at 14.5 eV instead of 15 eV.

Ref. [18]. For the energies of 18 and 20 eV the comparison between 45ch-SEP DCS results and experiments is similar to the 17ch-SEP and experiments for 11 eV. For 18 eV, at 0°, 90°, 135°, and 180°, the experimental datain Ref. [13] agree quite well with the 45ch-SEP calculation. Comparison among the results obtained in the 2ch-SEP, 17ch-SEP, and 45ch-SEP approximations inspires an intuition from classical physics: in a river with dam gates, as more gates are opened, the flux on each one decreases. Unfortunately, in this case, the use of 45 gates (channels) was not enough to provide the required flux into the state-resolved cross sections. Embedded in these results is the finding that for any system having a high density of energetically accessible states, as is the case for the molecule considered here, the rate of convergence of the multichannel coupling for electronically inelastic processes should be very slow. In order to overcome this difficulty and aiming at future applications using a redesigned computer code, we tested the possibility of defining a ficticious arbitrary threshold at 10 eV, meaning that all states opening up at energies between 10 and 18 eV were treated as degenerate open states with a threshold at 10 eV. Upon doing so, for the remaining 27 states (45 minus the ground state and the 17 excited states below 10 eV) we could use the same integrals (Coulomb potential integrals involving Cartesian Gaussians and plane waves) to evaluate the numerators and the Green function appearing in the expression for the scattering amplitude given by Eqs. (1) and (2). The use of the same on-shell energy for all these states decreases the number of integrals substantially. The results for this approximation are represented by the thin solid (blue) line in Figs. 1 and 3. For energies above 18 eV this approximation

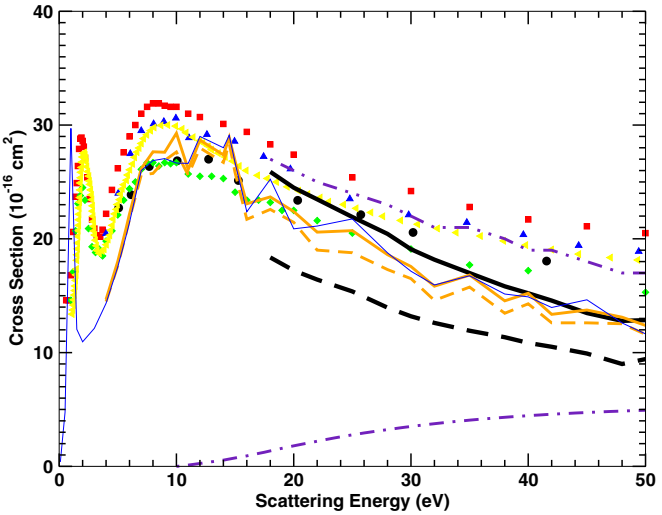

FIG. 4. (Color online) Total and integral cross sections for the energy region 0–50 eV. Thin solid (blue) line, 1-channel coupling plus polarization (the optical theorem gives the same result as the elastic transition); dashed (orange) line, elastic transitions for 2-channel coupling plus polarization; solid (orange) line, total cross section for 2-channel coupling plus polarization; thick dashed black line, elastic transitions for 45-channel coupling plus polarization; thick solid black line, total cross section for 45-channel coupling plus polarization; dot-dashed (indigo) line, ionization cross sections using the BEB aproximation; dot-dot-dashed (indigo) line, total cross sections for 45-channel coupling plus polarization plus ionization using the BEB approximation. Filled black circles, filled (red) squares, filled (green) diamonds, filled (blue) upward triangles, and filled (yellow) downward triangles: experiments of Refs. [1–5], respectively.

is quite satisfactory for the elastic and first triplet inelastic cases and it will be exploited for better convergence in channel coupling. At 15 eV (where channels that should be closed are now treated as open) the procedure based on the use of fictitious thresholds does not work as well. Figure 4 shows our calculated TCSs obtained through the use of the optical theorem, which is equivalent to the sum of the integral cross sections over all transitions $1 \rightarrow n$, from 1 to $N_{\rm open}$. In the 18- to 50-eV region, we see that the TCS for $N_{\rm open} = 45$ is not so different from $N_{\rm open} = 2$ or even $N_{\rm open} = 1$, but the effect on the elastic channel is quite clear, as one should expect by inspecting the corresponding DCSs. This reinforces the classical picture of the dam gates. The difference between DCSs given by our best calculation (the 45ch-SEP approximation) and the experimental data becomes larger as the energy increases. If the increment in the TCS is small with respect to the inclusion of more channels, this difference cannot be explained by the lack of these open channels. The disagreement is probably due to the ionization channels that are absent in our model. In order to check this point we estimate the ionization cross sections by using the BEB model and adding it to the elastic and inelastic contributions. As shown in Fig. 4 the resulting curve (elastic + inelastic + ionization) is in good agreement with the TCS results measured by different experimental groups [1–5]. Before concluding we need to discuss another important aspect of our calculations which is directly related to the convergence of the angular momentum in the expansion that is used to transform the scattering amplitude from body to laboratory frame.

V. ANGULAR MOMENTUM EXPANSION

In order to transform the scattering amplitude from the body-fixed frame (the reference frame best suited for carrying out the calculations) to the laboratory-fixed frame (the reference frame where the z axis is aligned with the direction of the incident wave vector, i.e., $\vec{k}_i = k_i \hat{z}$), we expand $\vec{k}_f$ in partial waves [28],

$$f(\mathbf{k}_f,\mathbf{k}_i) \equiv \langle \mathbf{k}_f | f | \mathbf{k}_i \rangle = \sum_{\ell=0}^{\ell_{\rm max}} \sum_{m=-\ell}^{\ell} \langle \mathbf{k}_f | \ell m \rangle \langle \ell m | f | \mathbf{k}_i \rangle, \quad (6)$$

where $\langle \mathbf{k}_f | \ell m \rangle$ is a spherical harmonic that can be easily converted from the body to the laboratory frame and $\langle \ell m | f | \mathbf{k}_i \rangle$ can be understood as the scattering amplitude of an electron entering the interaction region in a plane wave $|\mathbf{k}_i\rangle$ and leaving it in a partial wave $|\ell m\rangle$. Figure 5 shows the convergence of the DCS with respect to the paramenter $\ell_{\rm max}$, which represents the maximum angular momentum used in the expansion defined

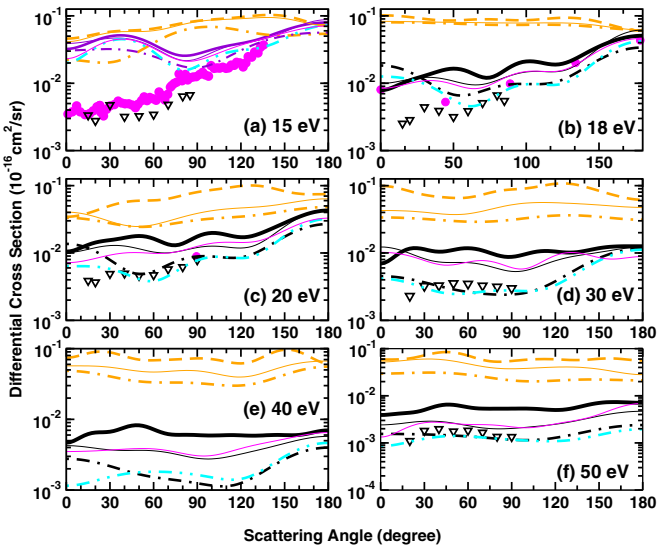

FIG. 5. (Color online) Outgoing angular momentum convergence in the differential cross sections for the $X\,^1A_g \rightarrow \tilde{a}\,^3B_{1u}$ electronic transition of the ethylene molecule for electron impact energies of (a) 15.0 eV, (b) 18.0 eV, (c) 20.0 eV, (d) 30.0 eV, (e) 40.0 eV, and (f) 50.0 eV. Short-dashed (orange) line, $\ell_{\rm max} = 10$, 2-channel coupling plus polarization; dashed-dotted (orange) line, $\ell_{\rm max} = 2$, 2-channel coupling plus polarization; thin solid (orange) line, $\ell_{\rm max} = 3$, 2-channel coupling plus polarization; short-dashed (violet) line, $\ell_{\rm max} = 10$, 17-channel coupling plus polarization; dashed-dotted (violet) line, $\ell_{\rm max} = 2$, 17-channel coupling plus polarization; short-dashed black line, $\ell_{\rm max} = 10$, 17-channel coupling plus polarization; dashed-dotted black line, $\ell_{\rm max} = 2$, 17-channel coupling plus polarization; thin solid black line, $\ell_{\rm max} = 3$, 17-channel coupling plus polarization; thick (cyan) dot-dot-dashed line, in and out angular momemtum representation with $\ell_{\rm max} = 3$, 17(45)-channel coupling plus polarization; thin solid (violet) line, in and out angular momentum representation with $\ell_{\rm max} = 4$, 17(45)-channel coupling plus polarization. Filled (magenta) circles and open black downward triangles: experiments of Refs. [13,18], respectively.

in Eq. (6). In this figure we present DCSs with $\ell_{\max} = 2, 3$, and 10 for the 2ch-SEP, 17ch-SEP, and 45ch-SEP approximations. Although not shown, for energies below 11 eV, the use of $\ell_{\max} = 2$ is enough to ensure convergence of the DCSs. At 15 and 18 eV the results are almost converged with $\ell_{\max} = 3$ and for energies of 20 eV and above we need to include more partial waves. Although not shown here, with the choice of $\ell_{\max} = 6$, DCSs in the entire energy region can be considered as sufficiently well converged. Compared with the experiments in Ref. [18] our DCSs are in reasonable agreement in magnitude for $\ell_{\max} = 2$ and in shape for $\ell_{\max} = 10$. Improving the results would require that, as we open more channels, the flux through the waves with $\ell \leqslant 2$ should remain as it is and the flux through the higher waves should decrease substantially. Although we have contributions from high partial waves in the scattering orbitals due to a multicenter expansion, we have only Cartesian Gaussians of the s, p, and d types on each center for carbon atoms, and on the hydrogen atoms we have only s and p types. This makes the description of the high partial waves more difficult and probably less accurate too.

Another way of calculating the scattering amplitude is by also expanding $\mathbf{k}_i$ in partial waves, so that now the DCSs are obtained with the following expression:

$$\langle \mathbf{k}_f | f | \mathbf{k}_i \rangle = \sum_{l=0}^{\ell_{\max}} \sum_{l'=0}^{\ell_{\max}} \langle \mathbf{k}_f | \ell m \rangle f(l,m;l',m') \langle l' m' | \mathbf{k}_i \rangle. \quad (7)$$

Here we note that, to the best of our knowledge, the complex Kohn and the R-matrix methods are limited to $\ell_{\max} = 4$, and in order to allow future comparisons, we have included results calculated from Eq. (7) with $\ell_{\max} = 3$ and 4. These results are represented in Fig. 5 by the thick dot-dot-dashed (blue) line and the thin solid (cyan) line, respectively. Although our DCSs obtained with $\ell_{\max} = 3$ show a nice agreement with experiment, it is important to note that it is not a converged calculation. For higher energies, more precisely, above 15 eV, where we expect a high-angular-momentum coupling, we also note that as we add open electronic states, the flux through these angular momenta waves decreases. This phenomenon may be due to the coupling with long-range Rydberg states that steal flux from the elastic and low-energy electronic states to properly describe their own high-angular-momentum coupling.

VI. CONCLUSIONS

In this work, we have obtained DCSs for electron elastic and electronically inelastic collisions with ethylene molecules according to the so-called N_{open}-channel-coupling scheme at the SEP approximation. More precisely, up to 45 states of ethylene obtained within a single-configuration-interaction representation of the target states were included in the open-channel space. This channel-coupling scheme enabled a detailed analysis of the influence of multichannel-coupling effects on the cross-section results. For elastic scattering the agreement with experimental data is quite good over the whole energy interval covered by the present study. Comparison among theoretical results obtained with different channel-coupling schemes clearly indicates that convergence of the elastic cross sections in terms of the number of excited states included in the open-channel space is relatively quickly achieved. For excitation of the $\tilde{a}\,^3B_{1u}$ state our calculations revealed that at 5.7 and 7 eV our results are in good agreement with the experiment. However, for energies above 7 eV our results lie systematically above the experimental data, indicating that perhaps more open channels would be needed in order to lower the magnitude of the computed inelastic DCSs. We also introduce a simple but rather effective method of representing multichannel-coupling effects through the use of fictitious thresholds and show that it provides DCSs in much better agreement with experiments.

ACKNOWLEDGMENTS

The present calculations were performed at IFGW-UNICAMP, LCPAD-UFPR, and LFTC-DFis-UFPR. M.H.F.B. acknowledges computational support from Prof. Carlos de Carvalho. The authors acknowledge support from the Brazilian agency Conselho Nacional de Desenvolvimento Científico e Tecnológico (CNPq). R.F.daC., M.T.doN.V., and E.M.O. acknowledge support from São Paulo Research Foundation.

[1] E. Brüche, Ann. Phys. (Leipzig) **394**, 909 (1929).
[2] K. Floeder, D. Fromme, W. Raith, A. Schwab, and G. Sinapius, J. Phys. B **18**, 3347 (1985).
[3] H. Nishimura and H. Tawara, J. Phys. B **24**, L363 (1991).
[4] C. Szmytkowski, S. Kwitnewski, and E. Ptasińska-Denga, Phys. Rev. A **68**, 032715 (2003).
[5] O. Sueka and S. Mori, J. Phys. B **19**, 4035 (1986).
[6] S. L. Lunt, J. Randell, J. P. Ziesel, G. Mrotzek, and D. Field, J. Phys. B **27**, 1407 (1994).
[7] B. Mapstone and W. R. Newell, J. Phys. B **25**, 491 (1992).
[8] R. Panajotovic, M. Kitajima, H. Tanaka, M. Jelisavcic, J. Lower, L. Campbell, M. J. Brunger, and S. J. Buckman, J. Phys. B **36**, 1615 (2003).
[9] M. A. Khakoo, K. Keane, C. Campbell, N. Guzman, and K. Hazlett, J. Phys. B **40**, 3601 (2007).
[10] C. S. Trevisan, A. E. Orel, and T. N. Rescigno, Phys. Rev. A **68**, 062707 (2003).
[11] C. Winstead, V. Mckoy, and M. H. F. Bettega, Phys. Rev. A **72**, 042721 (2005).
[12] R. F. da Costa, M. H. F. Bettega, and M. A. P. Lima, Phys. Rev. A **77**, 042723 (2008).
[13] M. Allan, C. Winstead, and V. McKoy, Phys. Rev. A **77**, 042715 (2008).
[14] R. F. da Costa, M. H. F. Bettega, and M. A. P. Lima, Phys. Rev. A **77**, 012717 (2008).
[15] R. F. da Costa, M. H. F. Bettega, M. A. P. Lima, M. C. A. Lopes, L. R. Hargreaves, G. Serna, and M. A. Khakoo, Phys. Rev. A **85**, 062706 (2012).

[16] T. N. Rescigno and B. I. Schneider, Phys. Rev. A **45**, 2894 (1992).
[17] Q. Sun, C. Winstead, V. McKoy, and M. A. P. Lima, J. Chem. Phys. **96**, 3531 (1992).
[18] T. P. T. Do, K. L. Nixon, M. Fuss, G. García, F. Blanco, and M. J. Brunger, J. Chem. Phys. **136**, 184313 (2012).
[19] K. Takatsuka and V. McKoy, Phys. Rev. A **24**, 2473 (1981); **30**, 1734 (1984).
[20] J. S. dos Santos, R. F. da Costa, and M. T. do N. Varella, J. Chem. Phys. **136**, 084307 (2012).
[21] M. H. F. Bettega, L. G. Ferreira, and M. A. P. Lima, Phys. Rev. A **47**, 1111 (1993).
[22] R. F. da Costa, F. J. da Paixão, and M. A. P. Lima, J. Phys. B **37**, L129 (2004).
[23] Y.-K. Kim and M. E. Rudd, Phys. Rev. A **50**, 3954 (1994).
[24] Y.-K. Kim, W. Hwang, N. M. Weinberger, M. A. Ali, and M. E. Rudd, J. Chem. Phys. **106**, 1026 (1997); M. A. Ali, Y.-K. Kim, W. Hwang, N. M. Weinberger, and M. E. Rudd, *ibid.* **106**, 9602 (1997); H. Nishimura, W. M. Huo, M. A. Ali, and Y.-K. Kim, *ibid.* **110**, 3811 (1999).
[25] M. W. Schmidt, K. K. Baldridge, J. A. Boatz, S. T. Elbert, M. S. Gordon, J. H. Jensen, S. Koseki, N. Matsunaga, K. A. Nguyen, S. J. Su, T. L. Windus, M. Dupuis, and J. A. Montgomery, J. Comput. Chem. **14**, 1347 (1993).
[26] C. C. Ballard, M. Hada, and H. Nakatsuji, Bull. Chem. Soc. Jpn. **69**, 1901 (1996).
[27] M. Kitajima, Y. Sakamoto, R. J. Gulley, M. Hoshino, J. C. Gibson, H. Tanaka, and S. J. Buckman, J. Phys. B **33**, 1687 (2000).
[28] M. A. P. Lima, T. L. Gibson, K. Takatsuka, and V. McKoy, Phys. Rev. A **30**, 1741 (1984).